NURETH14-388

VIPRE-W BENCHMARK WITH PSBT VOID AND TEMPERATURE TEST DATA

Y. Sung¹, R. L. Oelrich, Jr.¹ and C. C. Lee¹
N. Ruiz-Esquide², M. Gambetta², C. M. Mazufri²

¹ Westinghouse Electric Company LLC, Pittsburgh, Pennsylvania, U.S.A.

² INVAP, San Carlos de Bariloche, Argentina

sungy@westinghouse.com, oelricrl@westinghouse.com, leecc@westinghouse.com,
nruiz@invap.com.ar, gambetta@invap.com.ar, mazufri@invap.com.ar

Abstract

This paper summarizes comparisons of VIPRE-W thermal-hydraulic subchannel code predictions with measurements of fluid temperature and void from Pressurized Water Reactor subchannel and bundle tests. Using an existing turbulent mixing model, the empirical coefficient derived from code predictions in comparison to the fluid temperature measurement is similar to those from previous mixing tests of similar bundle configurations. The predicted steady state axial void distributions and time-dependent void profiles based on the Lellouche and Zolotar model generally agree well with the test data. The void model tends to predict lower void at the upper elevation under bulk boiling. The void predictions are in closer agreement with the measurements from the power increase, temperature increase and flow reduction transients than the depressurization transient.

1. Introduction

VIPRE-W (VIPREW or VIPRE) is Westinghouse version of the VIPRE-01* thermal-hydraulic subchannel code developed for light water reactor core design applications. The Penn State University (PSU) in cooperation with the Japan Nuclear Energy Safety Organization (JNES), under the sponsorship of the Organization for Economic Co-Operation and Development (OECD) and the United States Nuclear Regulatory Commission (USNRC), has developed benchmark exercises based on the Nuclear Power Engineering Corporation (NUPEC) Pressurized Water Reactor (PWR) subchannel and bundle tests (PSBT) [1]. The benchmark exercises include Phase I/Exercise 2 for the steady state void distributions, Phase I/Exercise 3 for the transient void distributions, and Phase II/Exercise 1 for the steady state fluid temperature distributions in the 5x5 rod bundles under PWR design conditions. This paper summarizes preliminary comparisons of VIPRE-W code predictions with the PSBT fluid temperature and void data.

^{*} VIPRE-01 is owned by Electric Power Research Institute, Palo Alto, California, U.S.A.

2. Test description

The PSBT problem specifications [1] provide a description of the NUPEC test facility and rod bundle designs. The test bundles were in 5x5 configurations for the void and exit temperature measurements, simulating a PWR 17x17 fuel assembly design with a fuel rod outside diameter (OD) of 9.5mm containing simple support and mixing vane (MV) grid spacers. The test section for the rod bundle void distribution measurement and an axial diagram indicating locations of grid spacers and pressure taps are shown in Figure 1. The effective heated length is 3658mm. Similar to rod bundle tests performed at the former Heat Transfer Research Facility (HTRF) in New York [2], the test rods were heated electrically using different wall thicknesses in order to create uniform or cosine axial power profiles. For example, the heater rods for the uniform axial power profile were made of Inconel 600 tubes with a wall thickness of 0.65mm. The tube inside was fit with an insulator tube made of Alumina having an OD of 8.2mm and an inside diameter (ID) of 5.8mm. Table 1 describes different test bundles used for the void and exit temperature measurements. For the void tests, the inner rods of a test bundle with the higher power were designated as "hot" rods, while the peripheral rods at lower power were "cold" rods. For the mixing test, the cold and hot rods were arranged in two columns on each side of the 5x5 test bundle, with three cold rods and two hot rods arranged alternatively in the central column. The test data were provided as part of the USNRC/OECD benchmark specifications [1].

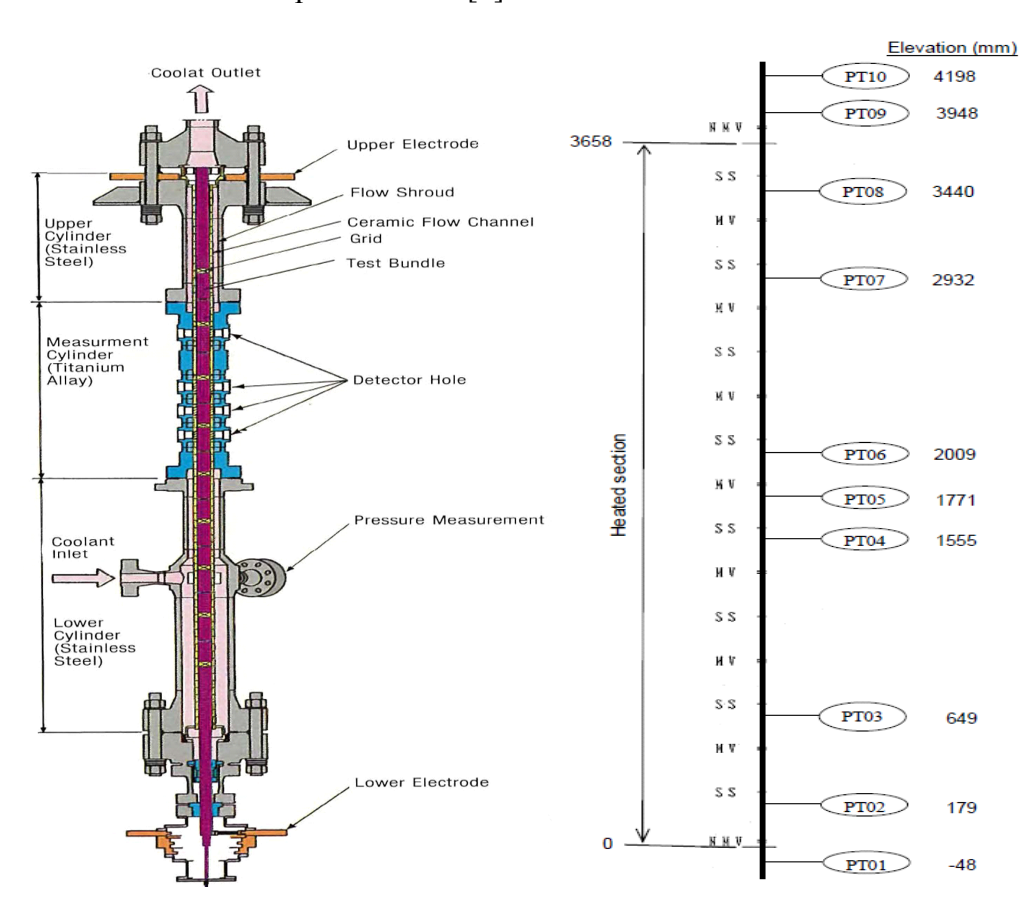


Figure 1 PSBT Test Section and Axial Diagram of Test Bundles [1]

Table 1 - Description of PSBT void and mixing tests

		,					
Parameter	B5	В6	В7	A1			
Number of Heated	25	25	24	25			
Rods							
Heated Rod (OD)	9.50	9.50	9.50	9.50			
(mm)							
Thimble Rod OD			12.24				
(mm)							
Rod-to-Rod Pitch	12.60	12.60	12.60	12.60			
(mm)							
Test Section Inner	64.9	64.9	64.9	64.9			
Width (mm)							
Axial Power Profile	Uniform	Cosine	Cosine	Uniform			
Hot/Cold Rod Power	1.00 / 0.85	1.00 / 0.85	1.00 / 0.85	1.00 / 0.25			
Ratio							
Grid Spacers and		7 Mixing Vane G	rid Spacers:				
Axial Elevations	4	71, 925, 1378, 1832,					
(mm)		2 Non-Mixing Vane	e Grid Spacers:				
		2.5, 375	55				
	8 Simple Support Grid Spacers:						
	237, 698, 1151, 1605, 2059, 2512, 2993, 3501						
Test Description	Steady state and	Steady state	Steady state	Steady state			
	transient void	and transient	and transient	mixing			
		void	void				

2.1 Mixing test

A fluid temperature test is often referred to as a mixing test, since it was designed to measure turbulent mixing effect in the bundle with a relatively large power gradient between hot and cold rods. In the PSBT mixing test (A1), thirty-six thermocouples were placed at the exit of each subchannel of the 5x5 test bundle for measuring fluid temperature. A total of 59 experimental data was taken from the test in the following range:

Parameters of Mixing Test	Range		
Pressure (bar)	49 - 166		
Mass Flux (10 ⁶ kg/m ² h)	0.44 - 17.08		
Inlet Temperature (°C)	84.5 - 289.2		
Bundle Power (MW)	0.11 - 3.44		

The mixing test was conducted mainly under the single-phase flow conditions.

2.2 Steady state void tests

The steady state void tests were performed with three different bundles, B5, B6 and B7, as described in Table 1. Seventy-four void distribution measurements were collected from each bundle in the following range:

Parameters of Void Tests	Range
Pressure (bar)	48.0 - 166
Mass Flux (10 ⁶ kg/m ² h)	2.0 - 15.
Inlet Temperature (°C)	143 - 322
Bundle Power (MW)	0.97 - 4.0
Void Fraction	0.0 - 0.80

A gamma-ray transmission method was used for measuring density of the flow, which was then converted to the void fraction of the vapor-liquid two-phase flow [1]. The measurements were taken at three elevations, 2216mm (Lower), 2669mm (Middle) and 3658mm (Upper). The measured data were averaged over the four central subchannels of the 5x5 test bundles.

A repeatability test was performed with another bundle, B8, similar to B5, with the uniform axial power profile and heated rods only (no guide thimble tube). A total of 31 matched pairs having similar test conditions of pressure, flow, inlet temperature and power were identified. The average differences (B8 – B5) in the test conditions and void measurements are given in Table 2. The matched pairs can be used for evaluating repeatability of the PSBT void test results.

Table 2 – Average differences between matched data pairs

	Measured Data			Testing Conditions			
Parameter	ΔVoid ΔVoid ΔVoid		Δ Pressure	ΔFlow	ΔTemperature	ΔPower	
(N = 31)	(lower)	(middle)	(upper)	(bar)	(10^6)	(°C)	(MW)
					kg/m ² h)		
Mean	0.011	0.062	0.022	0.516	0.035	-0.528	0.007
Standard							
Deviation	0.030	0.049	0.026	0.629	0.071	0.367	0.014

2.3 Transient void tests

Transient void tests were performed also with the three bundles, B5, B6 and B7, for four scenarios: power increase, flow reduction, depressurization, and inlet temperature increase. The initial conditions of the transient tests were set to be representative of PWR design conditions shown in Table 3. The void measurement technique was the same as that used for the steady state tests. Again, measurements were taken at three elevations, 2216 mm (Lower), 2669 mm (Middle) and 3658 mm (Upper). The measured data were averaged over the four central subchannels of the 5x5 test bundles.

The 14th International Topical Meeting on Nuclear Reactor Thermalhydraulics, NURETH-14 Toronto, Ontario, Canada, September 25-30, 2011

Test	Pressure	Mass Flux	Power	Inlet	Transients
Bundle	(bar)	$(10^6 \text{kg/m}^2 \text{h})$	(kW)	Temperature	
				(°C)	
	151.2	11.95	2282	300.4	Power
В5	150.8	11.93	2244	301.2	Flow
	150.0	11.92	2236	300.4	Pressure
	149.6	11.94	2230	301.7	Temperature
	155.1	11.55	2621	288.1	Power
В6	155.3	12.03	2574	288.8	Flow
	151.6	12.02	2556	288.2	Pressure
	154.2	11.92	2603	288.8	Temperature
	155.1	12.02	2500	291.9	Power
В7	155.0	12.04	2405	292.0	Flow
	152.0	11.99	2577	291.8	Pressure
	155.7	11.99	2496	290.2	Temperature

3. VIPRE-W code and modeling

VIPRE-W is an enhanced version of the VIPRE-01 subchannel code. VIPRE-01 was developed based on several versions of the COBRA code by the Battelle Pacific Northwest Laboratories for the Electric Power Research Institute (EPRI). It solves the finite difference equations for mass, energy, axial, and lateral momentum conservation for an interconnected array of channels, assuming incompressible and thermally expandable homogeneous flow. Although the formulation is homogeneous, empirical models are incorporated into the code to account for subcooled boiling and vapor/liquid slip in two-phase flow. Additional features of the VIPRE-W code include models for post-CHF fuel temperature calculations and fuel boiling duty evaluation at highly subcooled boiling conditions [4] and linkage to software libraries containing proprietary correlations and models. The new features enhance the code capability for PWR core design and licensing applications, but they do not alter the fundamental solution scheme of the VIPRE-01 code.

The VIPRE-W modeling of the test bundles is consistent with the benchmark specifications [1]. The radial geometric models are shown in Figure 2. The axial nodal length was set to be about 45.4 mm (1.8 inch). The two-phase flow model for comparison with the void data consisted of a profile fit subcooled and bulk boiling model developed by Lellouche and Zolotar [5] and the associated friction multiplier, also referred to as the EPRI void model [3]. It predicts the point of bubble departure from the heated surface under subcooled boiling and accounts for phase drift under bulk boiling. The EPRI void model was first selected for comparison with the PSBT data. Model sensitivity studies indicated that void predictions from other two-phase flow models in VIPRE-W may be in better agreement with the test data.

The turbulent mixing in subchannels was modeled using the following empirical correlation:

$$\Delta Q = -w' \times \Delta h \times \Delta X \tag{1}$$

where ΔQ = energy exchange due turbulent mixing (W or Btu/hr)

w' =lateral turbulent flow per unit length (kg/s/m or lbm/hr-ft)

 Δh = enthalpy difference between two subchannels (J/kg or Btu/lbm)

 ΔX = axial nodal length (m or ft)

$$w' = ABETA \times G_{AVG} \times S \tag{2}$$

where ABETA = empirical coefficient,

 G_{AVG} = average axial mass flow in the connected channels (kg/s/m² or lbm/s/ft²)

S = rod-to-rod gap width (m or ft)

ABETA is also referred to as Thermal Diffusion Coefficient (TDC) derived from mixing test data. Previous rod bundle mixing tests similar the PSBT test indicated that turbulent mixing is sensitive to spacing between two MV grids [6], while effect of simple support grids could be neglected. Since turbulent mixing increases with reduced grid spacing, in the VIPRE-W model ABETA was varied axially to account for the non-uniform MV grid spacings of the rod bundle.

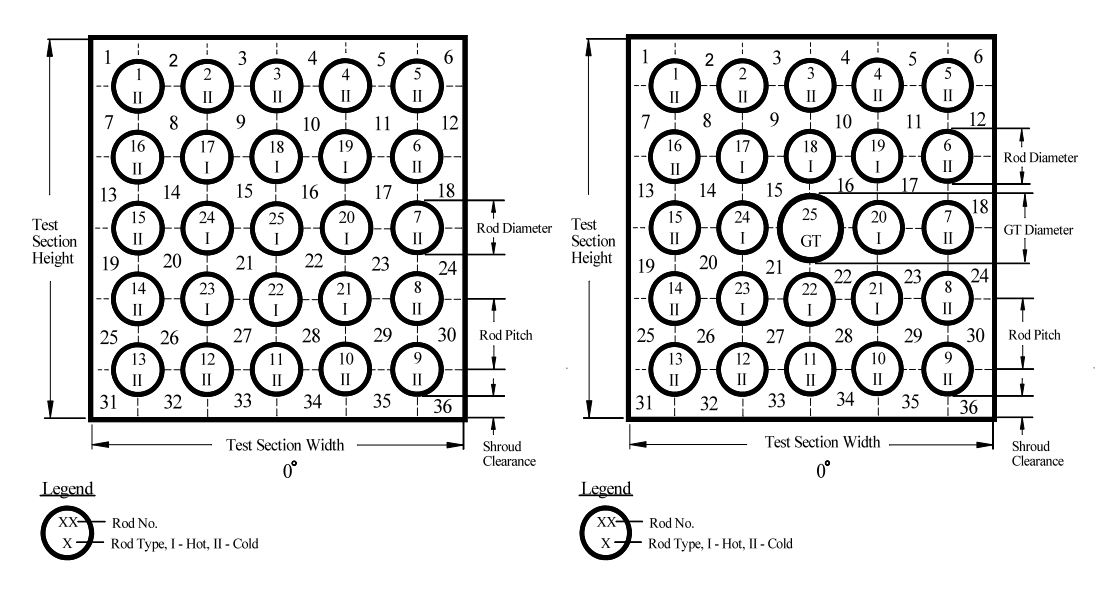


Figure 2 – VIPRE-W modeling of PSBT rod bundles

4. Exit temperature comparison

Each datum of the mixing test (A1) contains fluid temperature measurements at the top of the heated length or the channel exit. A VIPRE-W sensitivity study was performed with different values of ABETA in Equation 2. For each ABETA value, all test conditions are simulated yielding a set of subchannel exit temperature predictions. The predicted channel exit temperatures were then compared with the experimental data, in order to determine the best estimate ABETA value that yielded the smallest temperature differences. A figure of merit is defined to obtain the ABETA value which gives the best overall predictions: The squared

difference between measured and predicted temperature in each subchannel is averaged for each test and for each ABETA value selected in the study. The smaller the value is, the better the agreement between simulation and test data. Figure 3a shows that the temperature differences were relatively insensitive to ABETA varied in the range from 0.055 to 0.09. The best estimate ABETA value was found to be about 0.07 based on the test data from the heated rod and the grid spacer arrangements in the test bundle. As shown in Figure 3a, the estimated ABETA values remain unchanged if only the exit temperatures of the interior channels of the test bundle were taken into consideration, excluding the peripheral channels.

Figure 3b shows the average temperature differences in each channel. The temperature differences in the rod bundle appeared to be unevenly distributed. The hot rods of the mixing test were Rod No. 1, 2, 12 – 18, and 22 – 24 in Figure 2. The measured-to-predicted temperature differences were larger in the top half of the bundle (Channels 1 through 18 in Figure 2). Despite the uncertainty in the temperature differences, the thermal mixing coefficient (ABETA) of 0.07 from the PSBT mixing test is consistent with those values obtained from previous mixing tests of similar configurations [6]. The ABETA values in the VIPRE-W model varied with axial spacings between two MV grids in the test bundle.

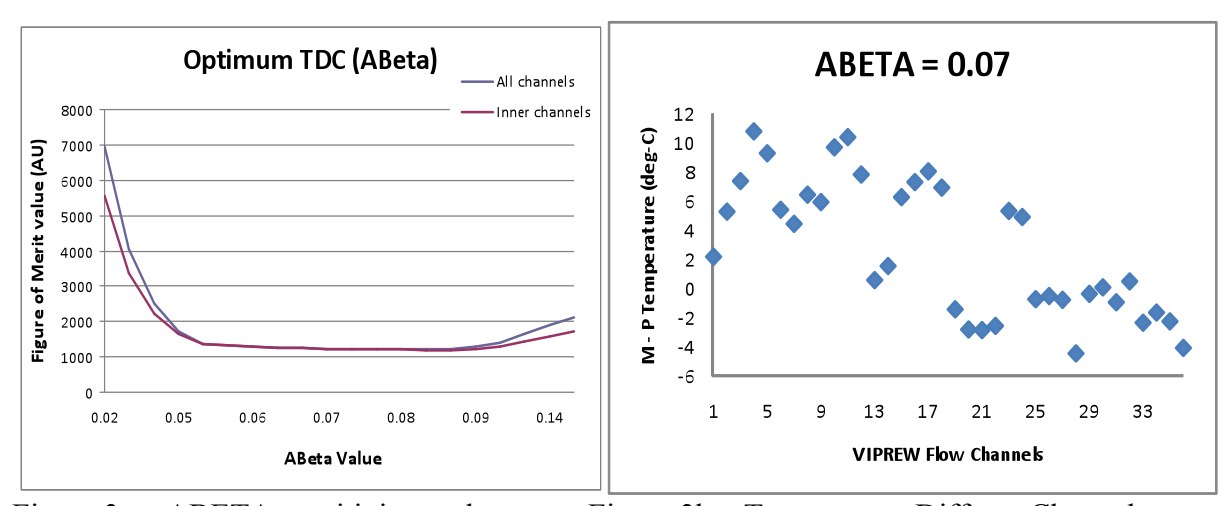


Figure 3a – ABETA sensitivity study

Figure 3b – Temperature Diff. vs. Channels

5. Steady state void comparison

The predicted void fractions from the central channels of the VIPRE-W model (Channels 15, 16, 21 and 22) in Figure 2 at the three elevations, 2216 mm (Lower), 2669 mm (Middle) and 3658 mm (Upper), were compared with the void measurements from the three tests, B5, B6 and B7. The comparisons based on the EPRI void model are summarized in Table 4.

Table 4 – Summary of steady state void comparison base on EPRI void model

		Measured – Predicted Void Fraction					
		Mean			Standard Deviation		
Bundle	Number	Lower	Middle	Upper	Lower	Middle	Upper

Test	of Points						
B5	74	-0.023	-0.022	0.031	0.029	0.046	0.039
B6	74	0.026	0.051	0.072	0.049	0.038	0.044
B7	74	-0.074	-0.043	0.019	0.035	0.044	0.028

There is no significant trend in the void differences with respect to the test conditions. However, the EPRI void model tends to under-predict the void under bulk boiling at the upper elevation in comparison to the measurements. The EPRI model was modified by combining the Lellouche and Zolotar subcooled void correlation with the homogeneous bulk boiling and two-phase flow friction multiplier. Table 5 indicates that the void predictions from the modified EPRI model are in better agreement with the data at the upper elevation.

Table 5 – Summary of steady state void comparison base on Modified EPRI void model

		Measured – Predicted Void Fraction					
		Mean			Sta	ndard Deviat	tion
Bundle	Number	Lower	Middle	Upper	Lower	Middle	Upper
Test	of Points						
B5	74	-0.025	-0.051	-0.018	0.032	0.058	0.054
В6	74	-0.029	-0.011	0.021	0.030	0.038	0.063
B7	74	-0.081	-0.080	-0.032	0.051	0.040	0.033

6. Transient void comparison

The VIPRE-W time-dependent calculations were performed using the modified EPRI void model (the Lellouche and Zolotar subcooled correlation combined with the homogeneous bulk boiling and two-phase flow friction multiplier) for the power increase, flow reduction, depressurization and temperature increase transients of the three test bundles. The predicted void fractions from the central channels of the VIPRE-W model at the three elevations were compared with the void measurements. The comparisons are shown in Figures 4 through 15 for the four transients of the three test bundles, B5T, B6T and B7T. The initial condition of each transient is listed in Table 3.

The predicted time-dependent void profiles are similar to the measured values. The predicted void values are in closer agreement with the measured values from the power increase, temperature increase and flow reduction transients than the depressurization transient. For the depressurization increase transients, the predicted values were generally lower at the upper elevation, although the magnitudes of the differences vary with the test bundles.

7. Conclusion

The mixing and void data from the PSBT benchmark exercises were evaluated using the VIPRE-W code. The turbulent mixing coefficient derived from code predictions in comparison to the mixing data is similar to those from previous mixing tests of similar bundle configurations. The predicted void fractions using the modified EPRI void model generally agree well with the steady state and transient void measurements, considering uncertainties in measurements and test

repeatability. Further sensitivity study and uncertainty evaluation are needed in order to understand the variations in the measured-to-predicted void differences among the test bundles.

8. References

- [1] A. Rubin, et al, "OECD/NRC benchmark based on NUPEC PWR subchannel and bundle tests (PSBT) Volume I: experimental database and final problem specifications," NEA/NSC/DOC(2010)1, US NRC/OECD Nuclear Energy Agency, November 2010.
- [2] C.F. Fighetti and D.G. Reddy, "Parametric Study of CHF Data," Volumes 1-3, NP-2609, Electric Power Research Institute, September 1982.
- [3] C.W. Stewart, et al, "VIPRE-01: A Thermal-Hydraulic Code for Reactor Cores," Volumes 1-3 (Revision 3, August 1989) and Volume 4 (April 1987), NP-2511-CCM-A, Electric Power Research Institute.
- [4] Y. Sung, et al, "Westinghouse VIPRE-01 applications for PWR core analyses," Ninth International Topical Meeting on Nuclear Reactor Thermal Hydraulics (NURETH-9), San Francisco, California, U.S.A., October 3-8, 1999.
- [5] G.S. Lellouche and B.A. Zolotar, "Mechanistic Model for Predicting Two-Phase Void Fraction for Water in Vertical Tubes, Channels and Rod Bundles," NP-2246-SR, 1982, Electric Power Research Institute.
- [6] F.F. Cadek et al, "Effect of Axial Spacing on Interchannel Thermal Mixing with the R Mixing Vane Grid," WCAP-7959-A, Westinghouse Electric Corporation, January 1975.

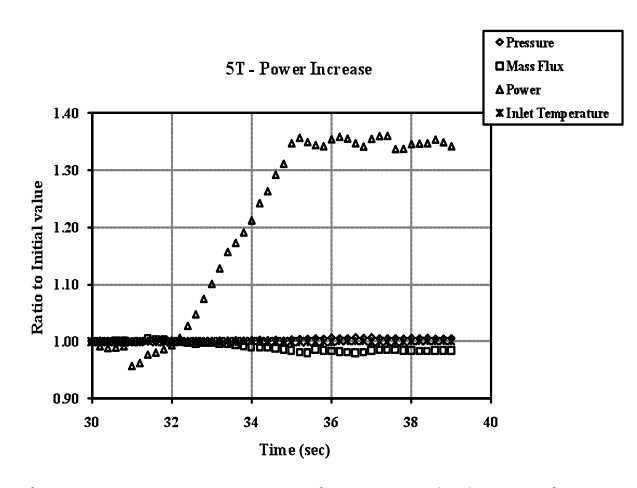


Figure 4a – B5T power increase (PI) transient

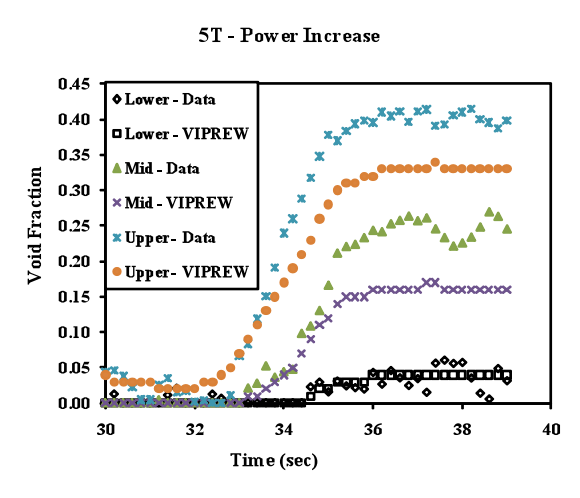


Figure 4b – B5T PI void comparison

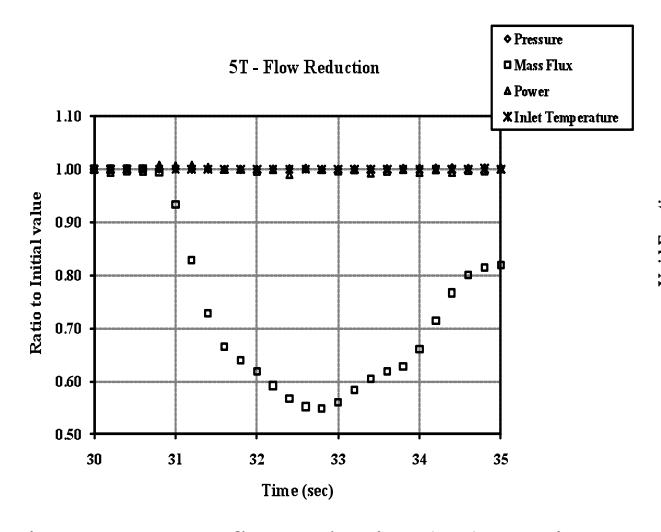


Figure 5a – B5T flow reduction (FR) transient

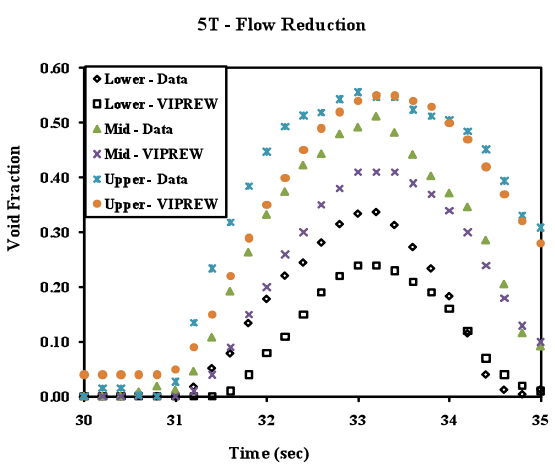


Figure 5b – B5T FR void comparison

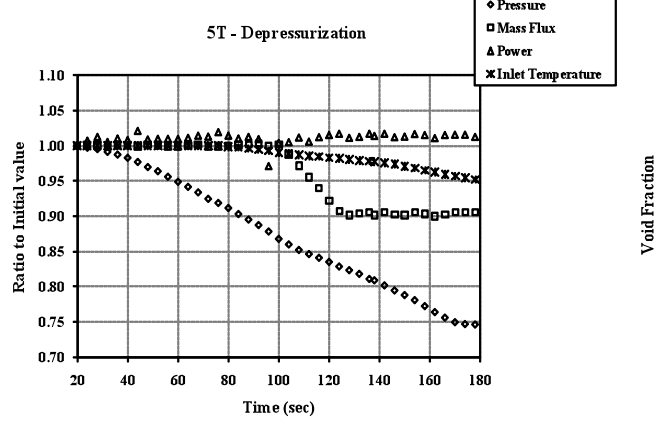


Figure 6a – B5T depressurization (DP) transient

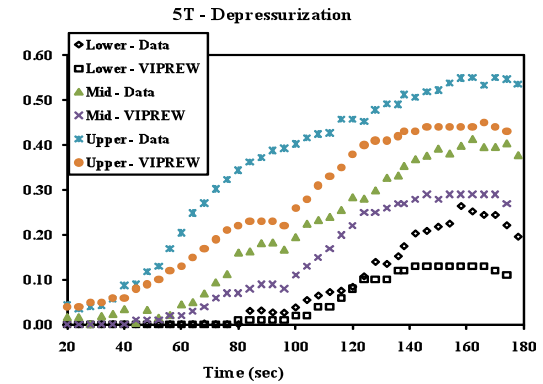


Figure 6b – B5T DP void comparison

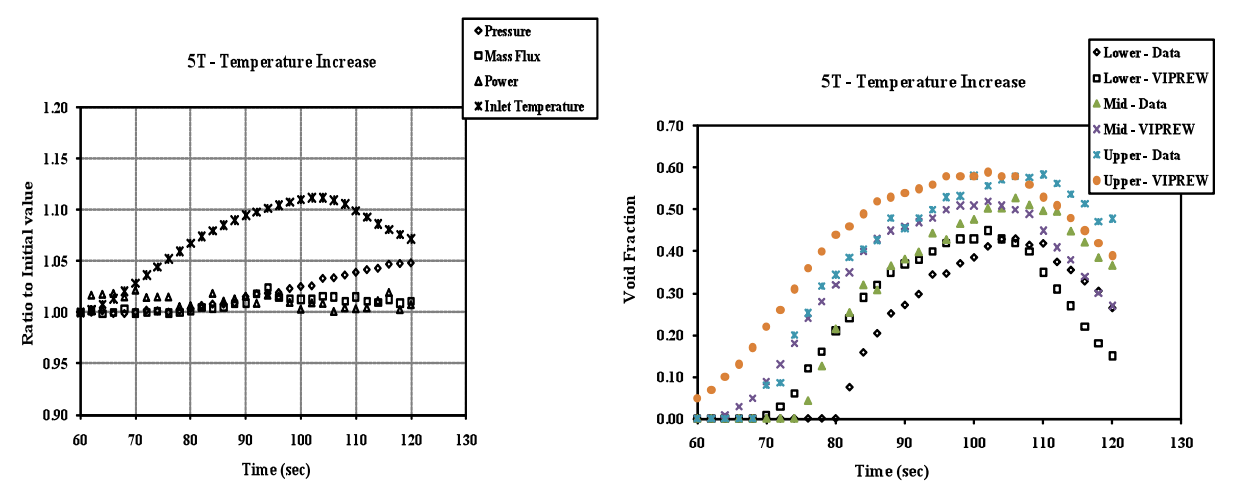


Figure 7a – B5T temperature increase (TI)

Figure 7b – B5T TI void comparison

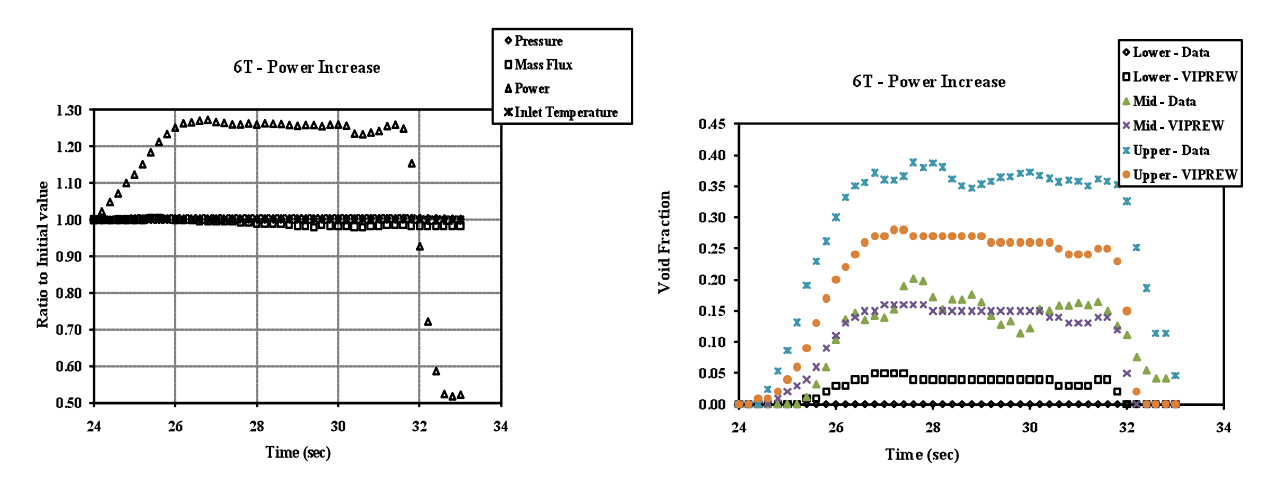


Figure 8a – B6T power increase (PI) transient

Figure 8b – B6T PI void comparison

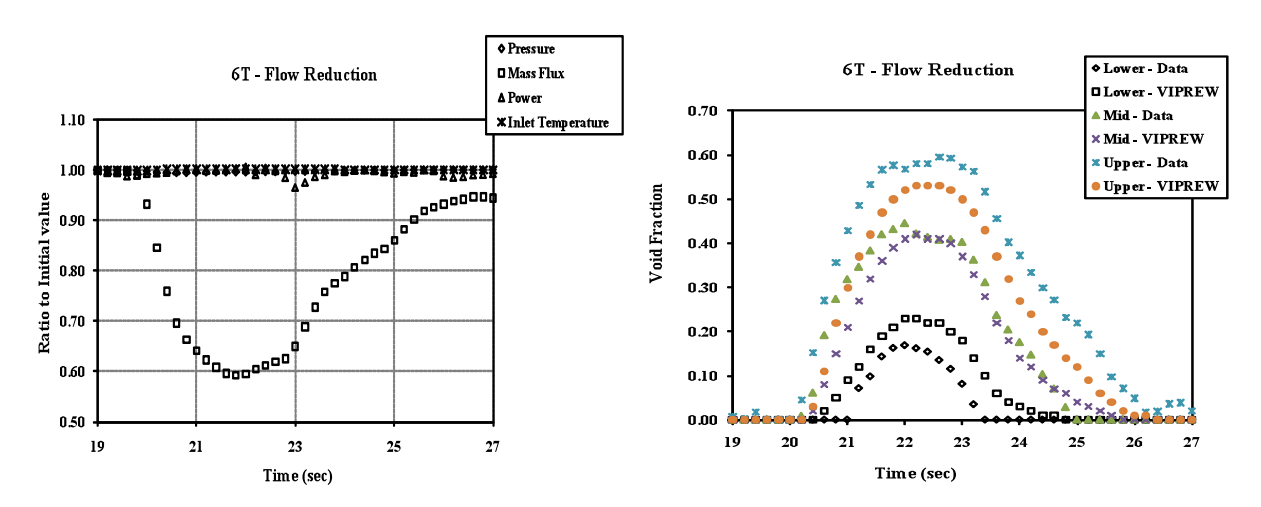
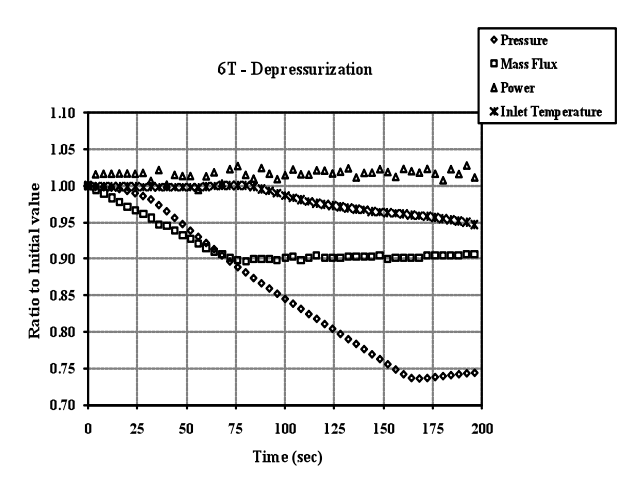


Figure 9a – B6T flow reduction (FR) transient

Figure 9b – B6T FR void comparison



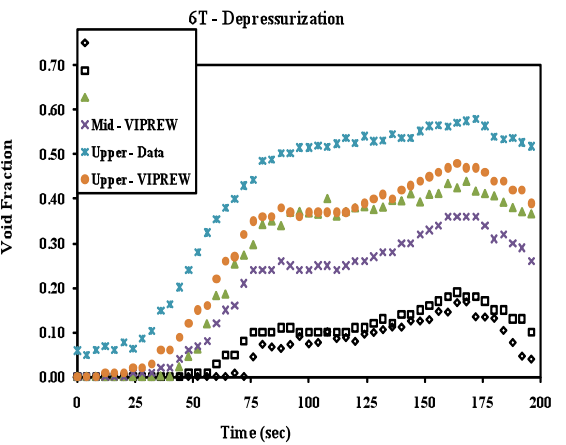
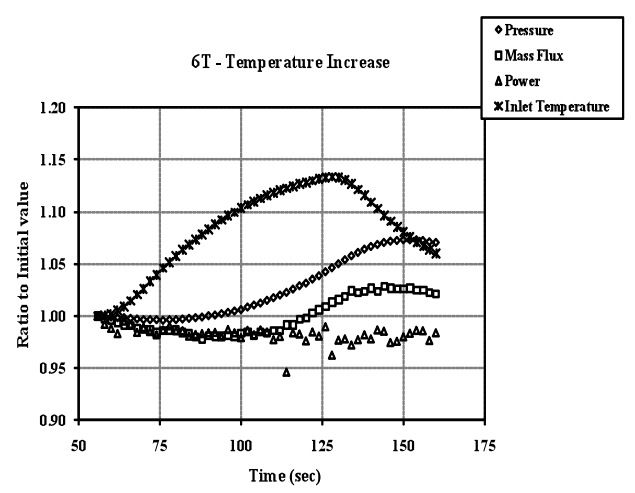


Figure 10a – B6T depressurization (DP) transient

Figure 10b – B6T DP void comparison



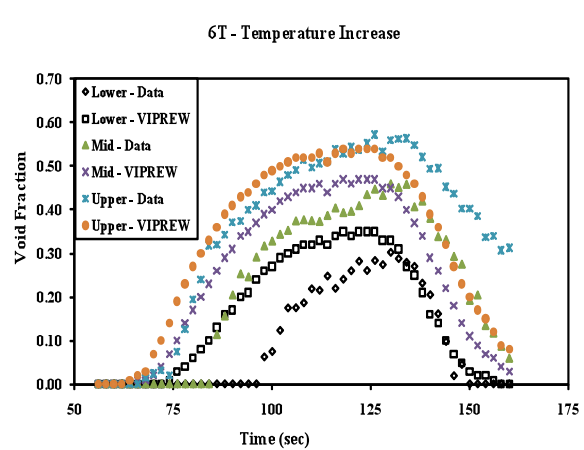
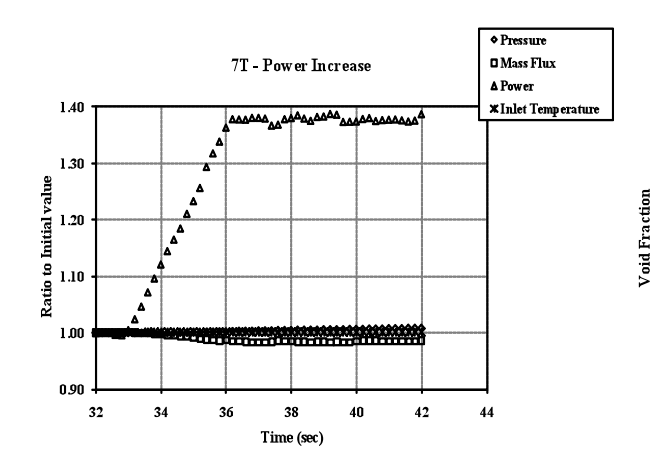


Figure 11a – B6T temperature increase (TI)

Figure 11b – B6T TI void comparison



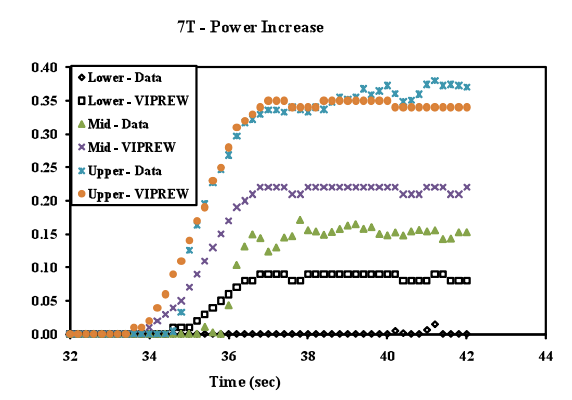


Figure 12a – B7T power increase (PI) transient

Figure 12b – B7T PI void comparison

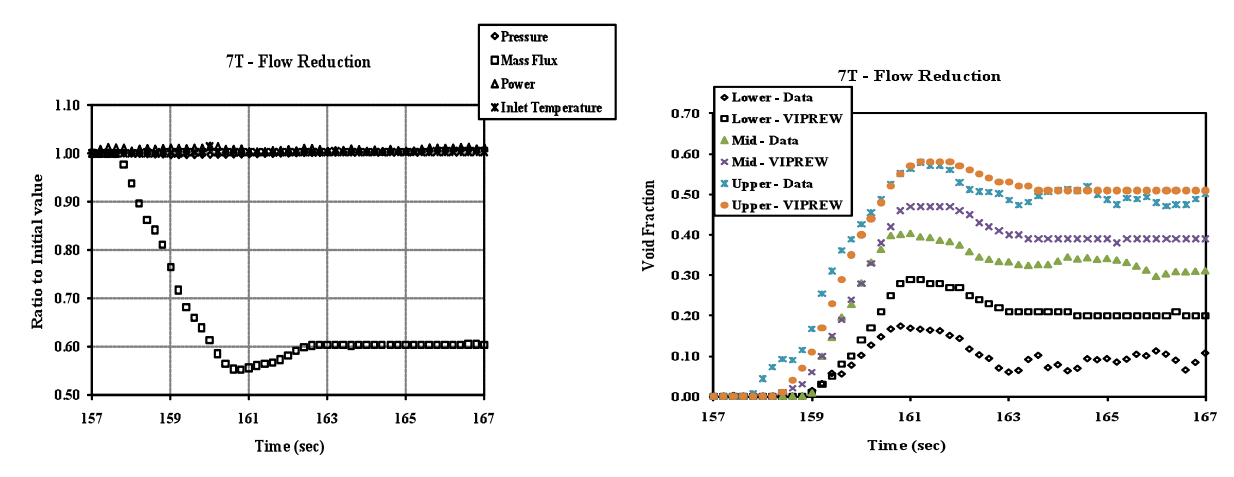


Figure 13a – B7T flow reduction (FR) transient

Figure 13b – B7T FR void comparison

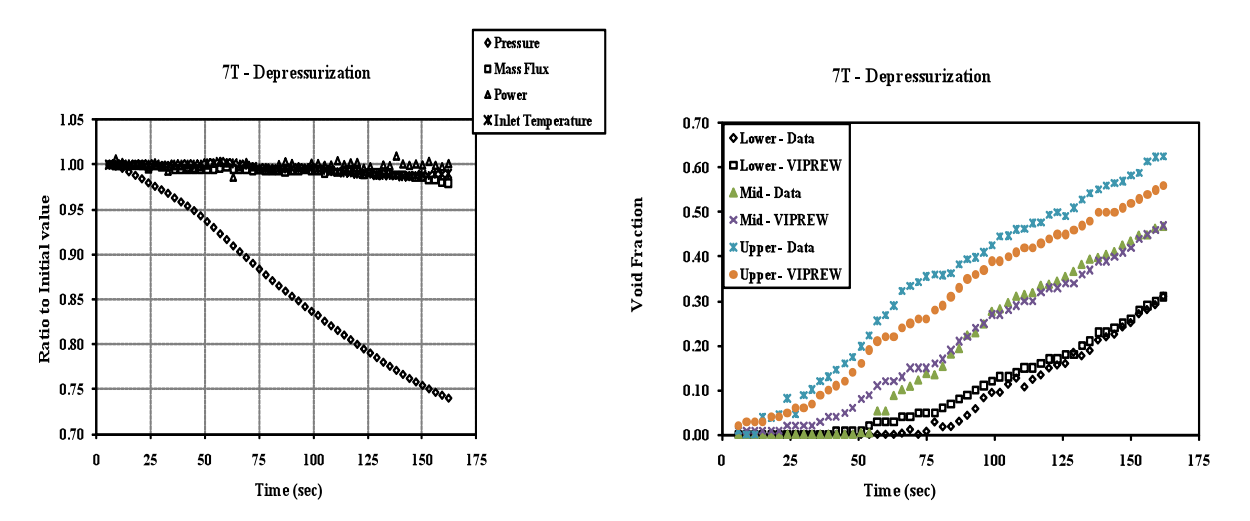


Figure 14a – B7T depressurization (DP) transient Figure 14a – B7T depressurization (DP) transient

Figure 14b – B7T DP void comparison

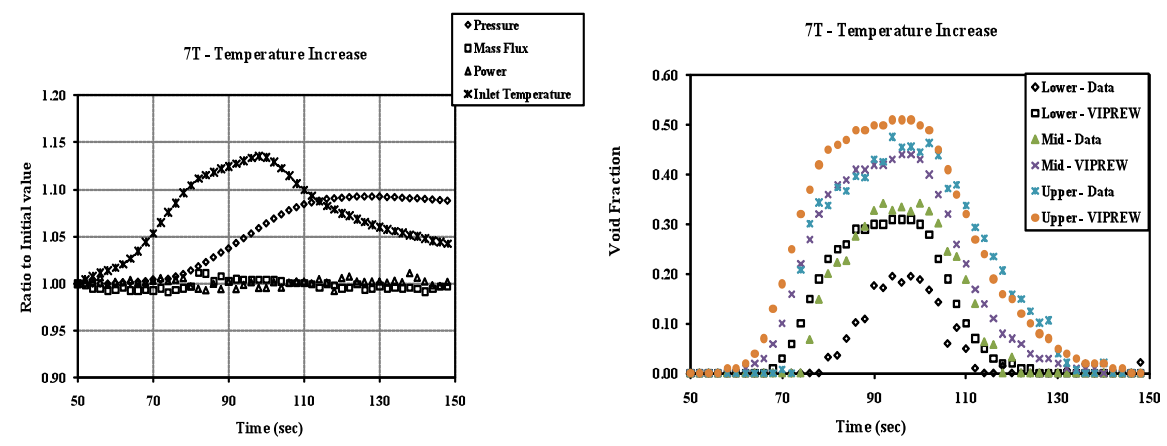


Figure 15a – B7T temperature increase (TI)

Figure 15b – B7T TI void comparison